Optimal Adaptive Linearizations of the AC Power Flow Equations

Sidhant Misra,[*] Daniel K. Molzahn,[†] and Krishnamurthy Dvijotham[‡]

Abstract—The power flow equations are at the heart of many optimization and control problems relevant to power systems. The non-linearity of these equations leads to computational challenges in solving power flow and optimal power flow problems (non-convergence, local optima, etc.). Accordingly, various linearization techniques, such as the DC power flow, are often used to approximate the power flow equations. In contrast to a wide variety of general linearization techniques in the power systems literature, this paper computes a linear approximation that is specific to a given power system and operating range of interest. An "adaptive linearization" developed using this approach minimizes the worst-case error between the output of the approximation and the actual non-linear power flow equations over the operating range of interest. To compute an adaptive linearization, this paper proposes a constraint generation algorithm that iterates between 1) using an optimization algorithm to identify a point that maximizes the error of the linearization at that iteration and 2) updating the linearization to minimize the worst-case error among all points identified thus far. This approach is tested on several IEEE test cases, with the results demonstrating up to a factor of four improvement in approximation error over linearizations based on a first-order Taylor approximation.

I. INTRODUCTION

The AC Power Flow (AC-PF) equations model the steady-state behavior of power systems and are therefore ubiquitous in problems relevant to planning and operations. The non-linearity of these equations poses significant computational challenges when used in many applications. Accordingly, simplified power flow models are commonly used instead of the AC-PF equations, the most popular among which are the DC approximation [1] in transmission systems and the LinDistFlow [2] in distribution systems. The literature includes many variants and related approaches for constructing power flow approximations [3]. Almost all of the existing approaches share one feature: they are designed for a general class of systems and operational conditions rather than being developed specifically for a particular system and operating range of interest. For instance, the DC power flow is appropriate for nearly lossless transmission networks operated with small phase angle differences and near-nominal voltage magnitudes. The quality of existing power flow approximations therefore depends on both the specifics of the operating condition and the application of interest, where one type of approximation error might be of more significance than others.

In contrast to existing approaches, this paper provides a framework for deriving computationally tractable approximations to the AC power flow equations that are both
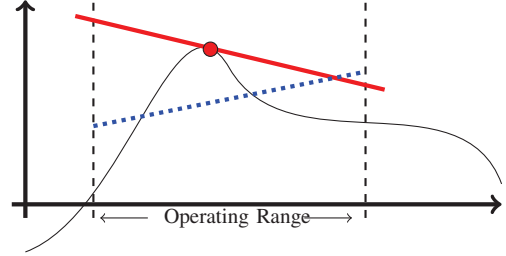
Fig. 1. Conceptual example comparing a linearization from a first-order Taylor approximation (solid red line) at a nominal operating point (red dot) and an adaptive linearization (dotted blue line) with a smaller worst-case error over the operating range.

- *adaptive* – tailored to be accurate around a given range of operating conditions for a specific system, and
- *optimal* – designed to minimize the error metric of interest to the application.

The power flow approximations from our approach are useful for a variety of applications. By restricting our search to tractable linear models, the approximations can be used in large optimization problems such as Optimal Power Flow (OPF) and on-line applications. Moreover, due to growing penetrations of renewable generation, Uncertainty Quantification (UQ) analyses are increasingly important in security assessment and operational planning under uncertainty through stochastic OPF (such as chance constrained [4]) formulations. In addition to their simple algebraic forms, the approximations we derive provide an explicit input–output relation (e.g., generation to line flows), as opposed to the implicit AC-PF equations, making them especially suitable for UQ analyses.

Regarding comparisons to alternative linearization approaches, Taylor approximation around a specified nominal operating point is *adaptive* and *optimal* in a limited sense: while forming the best linearization at the nominal point for a specific system, Taylor approximation is neither adaptive to nor optimal for operation in a *range around* the nominal operating point. Fig. 1 shows a conceptual example.

Other closely related work that considers a range of operation around a nominal point is proposed in [5], with extensions to three-phase systems in [6]. For each bus, the approach in [5] linearizes the relationship between the voltage phasor and the current injection phasor defined by the load model. When combined with the linear relationships between the voltage and current phasors dictated by the network equations, this approach yields a linear power flow approximation. Rather than a Taylor approximation around a single nominal operating point, the approach in [5] chooses a linearization of the load model that minimizes the least-square error for a predefined set of evenly distributed points near the nominal operating point. The resulting linearization is thus *adaptive* to the system and

operating range of interest. However, the set of points is not selected in any *optimal* manner to optimize some objective.

In other related work, [7] develops a linearization tailored to multiphase distribution networks, with associated theory regarding *a priori* error bounds on the predicted voltages. These bounds are appealing since they have an explicit form and are computationally inexpensive; however, they are limited in generality. Extending the analysis to consider voltage controlled ("PV") buses is not straightforward and may require significant theoretical extensions. Further, by only considering limits on the voltage magnitudes and power injections, the approach in [7] may be insufficient for fully capturing operating ranges with bounds on, e.g., phase angles and line flows.

In contrast to previous literature, our algorithm is both adaptive to a specified system and operating range as well as optimal in that the resulting linearization minimizes the worst-case error between the linearization and the AC-PF equations. While it is possible to consider other error metrics such as average error, worst-case error has the advantages of being simpler to compute and particularly relevant to problems where conservative estimates of system behavior are important. We compute this linearization by solving a "min–max" optimization problem that is constrained by the specific system model and operating range of interest. To tractably address this optimization problem, we employ an iterative constraint generation approach. Each iteration has two steps:

1) Find the point that maximizes the error between the previous iterate's linearization and the AC-PF equations.
2) Compute the best linear interpolation between the points found so far with respect to the worst-case error.

The algorithm terminates when the interpolation error in 2) is within a small tolerance of the maximum error in 1).

At the computational cost of repeated solution of optimization problems, our approach has the following advantages: 1) the linearizations minimize the error over the entire set of operating conditions, 2) the linearizations come with high-quality error bounds, 3) the formulation is very general, with straightforward extensions allowing for substantial flexibility in choosing the range of operating conditions, the desired error metric, the system and load models, input and output variables, etc. Empirical results demonstrate these advantages, including up to a factor of four improvement relative to the error resulting from a first-order Taylor approximation.

This paper is organized as follows. Section II overviews the AC power flow equations. Section III first formulates the "min–max" problem that defines the optimal adaptive linearizations and then presents our solution algorithm. Section IV discusses numerical results from application to several IEEE test cases. Section V concludes the paper.

II. OVERVIEW OF THE POWER FLOW EQUATIONS

The power flow equations model the steady-state relationship between the real and reactive power injections and the complex voltage phasors in a power system. We consider an n-bus power system with the sets of buses $\mathcal{B} = \{1, \ldots, n\}$ and lines $(l, m) \in \mathcal{L}$ (including both line terminals, i.e., if $(l, m) \in \mathcal{L}$, then $(m, l) \in \mathcal{L}$) with a fixed network topology.

Each bus $i \in \mathcal{B}$ has real and reactive power injections p_i and q_i as well as a complex voltage phasor with magnitude v_i and angle θ_i. Vectors of all the voltage magnitudes and angles are denoted $\mathbf{v}$ and $\boldsymbol{\theta}$. One bus is chosen to set the angle reference, $\theta_{ref} = 0°$. Each bus has a shunt admittance of $g_{sh,i} + jb_{sh,i}$, where $j = \sqrt{-1}$. Each line $(l, m) \in \mathcal{L}$ is modeled as a Π circuit with mutual admittance of $g_{lm} + jb_{lm}$ and shunt admittance $jb_{sh,lm}$. Our approach is also applicable to more general line models, such the MATPOWER [8] model that allows for off-nominal tap ratios and non-zero phase shifts.

With this notation, the AC-PF equations for real and reactive power flowing into line $(l, m) \in \mathcal{L}$ are

$$p_{lm} = g_{lm}v_l^2 - g_{lm}v_lv_m \cos(\theta_l - \theta_m) - b_{lm}v_lv_m \sin(\theta_l - \theta_m),$$
(1a)

$$q_{lm} = -(b_{lm} + b_{sh,lm}/2)v_l^2 + b_{lm}v_lv_m \cos(\theta_l - \theta_m)$$
$$- g_{lm}v_lv_m \sin(\theta_l - \theta_m).$$
(1b)

The AC-PF equations are completed by enforcing power balance at each bus $i \in \mathcal{B}$:

$$p_i = \sum_{\substack{(l,m)\in\mathcal{L} \\ \text{s.t. } l=i}} p_{lm} + \sum_{\substack{(l,m)\in\mathcal{L} \\ \text{s.t. } m=i}} p_{ml} + g_{sh,i}\,v_i^2,$$
(1c)

$$q_i = \sum_{\substack{(l,m)\in\mathcal{L} \\ \text{s.t. } l=i}} q_{lm} + \sum_{\substack{(l,m)\in\mathcal{L} \\ \text{s.t. } m=i}} q_{ml} - b_{sh,i}\,v_i^2.$$
(1d)

III. OPTIMAL ADAPTIVE APPROXIMATIONS

This section formulates the problem of finding optimal adaptive linearizations of the AC-PF equations and describes our solution algorithm.

A. Problem Formulation for Worst-Case Error Minimization

Given a range of operating conditions, we seek a linear approximation to the AC-PF equations that minimizes the magnitude of the worst-case error. In an abstract form, the optimization problem to compute this linearization is

$$\min_{\ell} \max_{x} \quad \text{error}(y^{AC}(x), y^{\mathbf{L}}(x; \ell))$$
(2a)

$$\text{s.t.} \quad \text{operational limits } x \in \mathcal{O}.$$
(2b)

Here x denotes the approximation's inputs (e.g., generation and load), ℓ denotes the parameters of the approximation that we seek to determine, $\text{error}(\cdot)$ denotes an appropriate error metric (e.g., the infinity norm), and $y^{AC}(x)$ and $y^{\mathbf{L}}(x; \ell)$ denote the corresponding values resulting from the AC-PF equations and the approximation, respectively, for the quantity of interest (e.g., the power flow on a given transmission line).

We now present a detailed version of (2). We assume that the range of operating conditions $\mathcal{O}$ is described by specified intervals for the real and reactive power production/consumption and the voltage magnitudes at each bus as well as intervals for the voltage angle differences across each line:

$$\mathcal{O} = \{(\mathbf{p}, \mathbf{q}, \mathbf{v}, \boldsymbol{\theta}) \mid \forall i \in \mathcal{B},\ \underline{p}_i \leq p_i \leq \bar{p}_i,$$
$$\underline{q}_i \leq q_i \leq \bar{q}_i,$$
$$\underline{v}_i \leq v_i \leq \bar{v}_i,$$
$$\forall (l, m) \in \mathcal{L},\quad \underline{\theta}_{lm} \leq \theta_l - \theta_m \leq \bar{\theta}_{lm},$$
$$(\mathbf{p}, \mathbf{q}, \mathbf{v}, \boldsymbol{\theta}) \text{ satisfy (1)}\}.$$
(3)

The notations $(\bar{\cdot})$ and $(\underline{\cdot})$ represent specified upper and lower bounds on the corresponding quantities.

Let y denote the quantity we want to approximate. Such quantities may include real and reactive power flows on the lines, current flows on the lines, voltage magnitudes at the buses, etc. We seek a linearization that relates a set of "independent" variables to the quantity of interest y. These independent variables are typically chosen to be controllable or specified quantities, e.g., real and reactive power injections, voltage magnitudes at generator buses, etc. For notational simplicity and to match typical practice, we form linear approximations for the real and reactive power flows on the lines, i.e., $y = p_{lm}$ and $y = q_{lm}$, with the real and reactive power injections, p_i and q_i, chosen as the independent variables. The formulation we detail in this paper is thus conceptually similar to "Power Transfer Distribution Factors" (PTDF) [9] in that both construct linear mappings from the power injections to the power flows on the lines. However, we emphasize that our approach is more general, with extensions to other quantities of interest and independent variables being conceptually trivial.

For some buses, such as those without any connected loads or generators, the operating conditions of interest may not allow any variation in the independent variables, i.e., $\underline{p}_i = \bar{p}_i$ and $\underline{q}_i = \bar{q}_i$ for our choice of power injections as the independent variables. We define these buses as *inactive*, with the remainder, denoted by the set $\mathcal{A} \subseteq \mathcal{B}$, defined as *active*.

Let ℓ_0 denote the constant term in the linear expression and let $\ell_{p,i}$ and $\ell_{q,i}$ denote the linear coefficients corresponding to the real and reactive power injection at bus $i \in \mathcal{B}$. Note that we only need to consider these coefficients for $i \in \mathcal{A}$ since the *inactive* buses have no variation in power injections and are therefore implicitly included in the constant term ℓ_0. We denote the vectors containing the coefficents as $\boldsymbol{\ell}_p$ and $\boldsymbol{\ell}_q$, respectively. The collection of coefficients $\mathbf{L} = (\ell_0, \boldsymbol{\ell}_p, \boldsymbol{\ell}_q)$ defines a linear approximation for y:

$$y \approx y^{\mathbf{L}} = \ell_0 + \sum_{i \in \mathcal{A}} \ell_{p,i}\, p_i + \sum_{i \in \mathcal{A}} \ell_{q,i}\, q_i. \quad (4)$$

The worst-case absolute error for a specified linearization $\mathbf{L}$ over the operating conditions defined by $\mathcal{O}$ is given by the maximum of the error in the positive and negative directions:

$$z^+(\mathbf{L}) \text{ (or } z^-) = \max_{\mathbf{p},\mathbf{q},\mathbf{v},\boldsymbol{\theta}} \quad y^{\mathbf{L}} - y \quad (\text{or } y - y^{\mathbf{L}}) \quad (5a)$$

$$\text{s.t.} \quad y^{\mathbf{L}} = \ell_0 + \sum_{i \in \mathcal{A}} \ell_{p,i}\, p_i + \sum_{i \in \mathcal{A}} \ell_{q,i}\, q_i, \quad (5b)$$

$$(\mathbf{p}, \mathbf{q}, \mathbf{v}, \boldsymbol{\theta}) \in \mathcal{O}. \quad (5c)$$

The problem of finding the optimal linear approximation can then be cast as a "min–max" problem:

$$\min \quad z \quad (6a)$$

$$\text{s.t.} \quad z \geq z^+, \qquad z \geq z^-, \quad (6b)$$

$$\text{Equations defining } z^+ \text{ and } z^- \text{ (5).} \quad (6c)$$

The inner maximization is implicitly contained in (6c).

Each solution to (6) gives a linearization for one quantity of interest, y. Obtaining linearizations for multiple quantities of interest (e.g., the real and reactive power flows on *every* line)

is accomplished by repeatedly solving (6). Since the linearizations for each quantity of interest are computed independently, the computations can be trivially parallelized.

B. Constraint Generation Algorithm

Constraint generation algorithms are popular choices for solving robust optimization (or "min–max") problems. Accordingly, this section describes a constraint generation algorithm for solving the bilevel optimization problem (6).

ALGORITHM: **FindOptLin**

Step 1: *(Initialization)* Choose an initial set of scenarios $\mathcal{S}$. Each scenario $s \in S$ corresponds to a specific set of values for $(\mathbf{p}(s), \mathbf{q}(s), \mathbf{v}(s), \boldsymbol{\theta}(s)) \in \mathcal{O}$.

Step 2: *(Find best linear approximation)* Find the linearization $\mathbf{L}$ that minimizes the worst-case approximation error for the scenarios in $\mathcal{S}$ by solving the following Linear Program (LP):

$$z_* = \min_{\ell_0, \boldsymbol{\ell}_p, \boldsymbol{\ell}_q} \quad z \quad (7a)$$

$$\text{s.t.} \quad (\forall s \in \mathcal{S})$$

$$z \geq \left(\ell_0 + \sum_{i \in \mathcal{A}} \ell_{p,i}\, p_i(s) + \sum_{i \in \mathcal{A}} \ell_{q,i}\, q_i(s) \right) - y(s), \quad (7b)$$

$$z \geq y(s) - \left(\ell_0 + \sum_{i \in \mathcal{A}} \ell_{p,i}\, p_i(s) + \sum_{i \in \mathcal{A}} \ell_{q,i}\, q_i(s) \right), \quad (7c)$$

where $y(s)$ is the value of y satisfying the AC-PF equations (1) in scenario s. Since (7) is a relaxation of (6), z_* lower bounds the objective of (6).

Step 3: *(Find the worst-case error)* Solve (5) to obtain the worst-case positive and negative errors $z^+(\mathbf{L})$ and $z^-(\mathbf{L})$ and the corresponding worst-case scenarios s^+ and s^-. Note that $z^* = \max\{z^+(\mathbf{L}), z^-(\mathbf{L})\}$ upper bounds the objective of (6).

Step 4: *(Check stopping criterion)* If the upper and lower bounds are close, i.e., $z^* - z_* < \epsilon$ where $\epsilon > 0$ is a tolerance parameter, then terminate and declare $\mathbf{L}$ as the optimal linear approximation of the AC-PF equations over $\mathcal{O}$. Otherwise, if $z_* < z^+(\mathbf{L}) - \epsilon$ and/or $z_* < z^-(\mathbf{L}) - \epsilon$, add the corresponding scenarios, s^+ and/or s^-, to $\mathcal{S}$ and go to *Step 2*.

C. Discussion

We next discuss various aspects of the problem formulation (6) and solution approach.

1) Interpretation as an Improvement to the First-Order Taylor Approximation: Both our linearization and the commonly used PTDF approximation model linear relationships between the power injections at the buses and the power flows on the lines. When constructed using the power flow Jacobian evaluated at a nominal operating point, the "AC-PTDF" matrix [9] is closely related to the first-order Taylor approximation of this relationship. Thus, the AC-PTDF matrix provides the optimal linear approximation *at* the nominal operating point. However, the linearization associated with the AC-PTDF matrix is not necessarily optimal in the sense of (6) for operational conditions in a range $\mathcal{O}$ *around* the nominal operating point.

The output of the constraint generation algorithm should approach the AC-PTDF linearization as the operating range $\mathcal{O}$ shrinks. As shown in Fig. 5, our numerical results corroborate this expected behavior: when considering a small enough range $\mathcal{O}$, the coefficient values for $\boldsymbol{\ell}_p$ and $\boldsymbol{\ell}_q$ match those of the AC-PTDF matrix within the algorithm's tolerance ϵ. The coefficient values start to deviate from those of the AC-PTDF matrix as the range of operation increases. Accordingly, an interpretation of our linearizations is that they "adjust" the AC-PTDF matrix to consider a broader operating range than the single point used to construct the AC-PTDF matrix.

2) Generality of the Formulation: The problem formulation and system model in Section III-A can be modified in a variety of ways. Ongoing work focuses on the following generalizations and other related ideas.

a) Operating Conditions: The operating range $\mathcal{O}$ can be modified to best represent the expected generations and demands by changing problem (7). For instance, one could consider generator capability curves [10] and various load models such as constant power factor load variation, ZIP models [11], induction machine models [12], etc.

b) Linearization Coefficients: The formulation detailed in this paper constructs a linear approximation of the quantity y (real and reactive power flows on the lines) expressed in terms of real and reactive power injections at the buses. Other choices of variables can easily be accommodated (e.g., a PV bus i can be modeled via a voltage magnitude coefficient $\ell_{v,i}$ instead of a reactive power coefficient $\ell_{q,i}$).

c) System Models: While this paper considers a balanced single-phase equivalent network model, the proposed approach is extensible to more general system models, such as unbalanced three-phase representations suitable for modeling distribution networks. Our approach could even be applied to black-box models of system behavior, such as the output of a detailed simulation, provided that there is some method reminiscent of (5) for estimating worst-case scenarios.

d) Error Metrics: The worst-case error formulated in this paper is one of many possible error metrics. By modifying the objectives of (5) and (7), other error metrics could be considered. Weighted norms are particularly relevant to applications where the impact of errors is asymmetric (i.e., underestimation of errors is more harmful than overestimation or vice-versa).

3) Computational Complexity: Each iteration of the *FindOptLin* algorithm solves the LP in (7) and the Non-Linear Program (NLP) in (5). The LP in (7) can be interpreted as a relaxation of the formulation in (6). The model is then iteratively tightened in *Step 3* by augmenting the set of scenarios $\mathcal{S}$. Given the capabilities of LP solvers, (7) is solved very quickly in each iteration. Consequently, most of the computational burden comes from computing the worst-case scenarios in (5), with two NLP solves required per iteration.

As shown by the results in Section IV, the constraint generation algorithm *FindOptLin* finds linearizations $\mathbf{L} = (\ell_0, \boldsymbol{\ell}_p, \boldsymbol{\ell}_q)$ for the real and reactive flows on each line for the considered systems in reasonable computation times (ranging from a few seconds up to a minute per line). A variety of improvements could enable application to larger systems. For instance, the problem is trivially parallelizable over both the variables of

interest y and the two NLP optimization problems (5) solved at each iteration. Moreover, the number of variables that need to be approximated is small in many applications (e.g., the relatively few "monitored lines" in OPF problems). This limits the number of times that the algorithm *FindOptLin* needs to be evaluated. Furthermore, since intermediate iterations often provide reasonable accuracy (see the convergence characteristics in Fig. 2), the coefficient values from an intermediate iteration could be used rather than waiting for convergence (or, equivalently, a large tolerance may be acceptable). Finally, since initial numerical experience suggests that the worst-case error increases slowly with larger operating ranges, the linearizations could be computed off-line for a wide range of possible operating conditions $\mathcal{O}$, with the resulting models used in on-line applications. Future work will further discuss computational tractability and various improvements.

4) Guaranteed Bounds on Approximation Errors: The performance of the *FindOptLin* algorithm strongly depends on the quality of the solutions to the non-convex problem (5). Local solvers such as Ipopt [13] are often capable of finding local optima of (5). While lacking guarantees regarding global optimality, previous experience with related problems [14] as well as a variety of numerical experiments suggests that the solutions obtained from local solvers are often close to the global optimum, if not, in fact, globally optimal. Furthermore, most of the computational burden of the *FindOptLin* algorithm is attributable to (5). Local solution algorithms such as Ipopt are often substantially faster than global solution algorithms.

For these reasons, we apply Ipopt to the subproblems (5). The approximation error bounds directly computed from these subproblems therefore lack rigorous guarantees. However, once the *FindOptLin* algorithm converges, it is possible to compute the exact worst-case linearization error *a posteriori* using a global solver or an upper bound on the worst-case error using a convex relaxation of the AC-PF equations in (5). We specifically apply a convex relaxation consisting of the second-order complex moment/sum-of-squares relaxation [15] in combination with the QC relaxation [16], [17] and bound tightening techniques [17]. As shown in Fig. 4, the empirical results from this relaxation demonstrate that the error bounds obtained from the local solver are at least reasonably close to the true worst-case errors. Ongoing work seeks to compare the impact of applying a convex relaxation versus a local solver to the subproblems (5) when evaluating *FindOptLin*.

IV. TEST CASE RESULTS

This section applies *FindOptLin* to several test cases from [18] and analyzes the errors for the resulting approximations. For comparison purposes, we use the first-order Taylor approximation (i.e., the linearization corresponding to the AC-PTDF matrix evaluated at the nominal operating point).

The implementation is written in Julia language using the PowerModels [19] and JuMP [20] modeling packages. We use Gurobi as the LP solver and Ipopt [13] as the NLP solver.

A. Behavior of the Algorithm

Fig. 2 shows a typical evolution of the objective values in the LP (*Step 2*) and NLP (*Step 3*) in each iteration of our
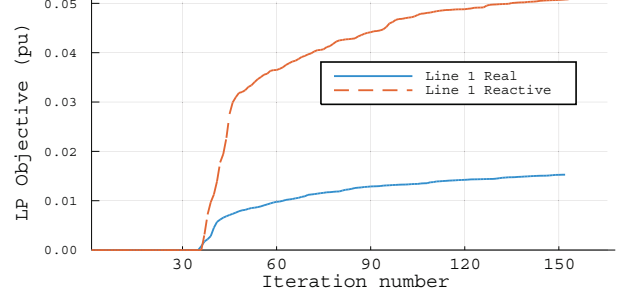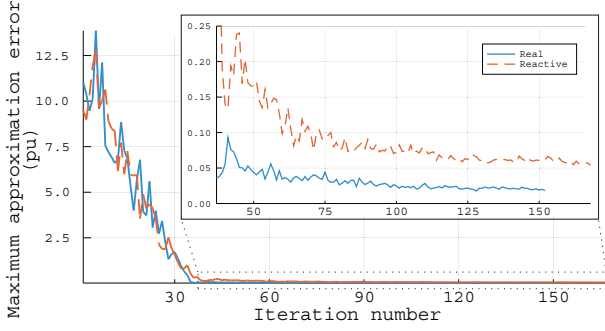
Fig. 2. The maximum linearization error from solving (5) (left) and the objective of the LP relaxation (7) (right) as a function of the iterations of *FindOptLin* for the IEEE RTS 96 test case. The results are plotted for line 1 with $R = 30\%$. The left figure shows a zoomed view of the "convergence phase".

algorithm for the IEEE RTS 96 test case. The LP's objective in *Step 2* is monotonically increasing, which is consistent with the fact that each iteration of *FindOptLin* tightens the LP's feasible space by adding constraints corresponding to the new scenarios discovered in the previous iteration's *Step 3*. The non-monotonic behavior of the NLP's objective function reveals two distinct phases. The first is an *exploration phase* (e.g., iterations 1-32 in Fig. 2) where the coefficients of the linear approximation are far from their optimal values. This phase has significant changes in both the worst-case error and the coefficients of the linear approximation across iterations. The second is a *convergence phase* (the iterations after 32 in Fig. 2) where the coefficients have small fluctuations across iterations as they converge to their optimal values.

Curiously, the start of the convergence phase coincides with the objective of the LP first taking positive values. This suggests that scenarios from the exploration phase eliminate overly optimistic linear approximations. Moreover, this indicates potential advantages from "warm-starting" the algorithm by, e.g., initializing $\mathcal{S}$ with the worst-case scenarios computed for first-order Taylor approximations at various feasible points.

Most of the iterations are spent in the convergence phase. This is likely due to the fact that the algorithm *FindOptLin* is a first-order method, which are known to often suffer from slow convergence rates. As a subject for future work, this suggests that applying a second-order method after the exploration phase could significantly speed computations.

B. Analysis of Approximation Error

To evaluate the accuracy of the optimal adaptive approximations, we compare the worst-case approximation error for varying sizes of the operating region $\mathcal{O}$. We first solve an AC OPF problem to obtain a nominal operating point with power injections denoted by $(\mathbf{p}^*, \mathbf{q}^*)$. We then use a *radius R* to control the size of the operating region $\mathcal{O}_R$:

$$
\begin{aligned}
\mathcal{O}_R = \{ &(\mathbf{p}, \mathbf{q}, \mathbf{v}, \boldsymbol{\theta}) \mid \\
&(1 - R)(\mathbf{p}^*, \mathbf{q}^*) \leq (\mathbf{p}, \mathbf{q}) \leq (1 + R)(\mathbf{p}^*, \mathbf{q}^*), \\
&\underline{\mathbf{v}} \leq \mathbf{v} \leq \bar{\mathbf{v}}, \\
&\underline{\theta}_{lm} \leq \theta_l - \theta_m \leq \bar{\theta}_{lm}, \ \forall \, (l, m) \in \mathcal{L}, \\
&(\mathbf{p}, \mathbf{q}, \mathbf{v}, \boldsymbol{\theta}) \text{ satisfy (1)} \}.
\end{aligned}
\tag{8}
$$

This choice of $\mathcal{O}_R$ allows both the generation and the load to vary within a certain percentage of their nominal values.

Fig. 3 shows the worst-case errors for lines 1 and 18 in the IEEE RTS 96 test case. The errors for the first-order Taylor approximation (i.e., using the AC-PTDF matrices) are also included. These results represent typical cases for which the approximation errors are relatively large (line 18) and small (line 1). The figure shows the advantage of our approach. For a radius $R = 40\%$, the optimal approximation shows a significant improvement in the approximation error (roughly a factor of four) over the first-order Taylor approximation.

Consistent with our other numerical experiments, the approximation errors for reactive power are worse than those for real power. We also note that there is no correlation evident between the quality of the approximations for the real and reactive power flows on a given line. While the approximation for the real power on line number 1 is quite accurate for both the optimal linearization and the Taylor approximation, the same does not hold for reactive power approximation.

As discussed in Section III-C4, convex relaxation techniques can be used to evaluate the quality of the the worst-case errors computed by the local solver. For the optimal linearization resulting from applying *FindOptLin* to the IEEE RTS 96 test case with a radius of 40%, Fig. 4 compares the worst-case errors from locally solving (5) to the bounds on the worst-case errors from a relaxation of (5). As discussed previously, we use a relaxation formed from a combination of the techniques in [15]–[17]. These results as well as the relaxation bounds for other test cases demonstrate that the worst-case errors from the local solver are at least near the actual worst-case errors (i.e., the local solutions to (5) are at least close to being globally optimal). Note that the optimality gaps in Fig. 4 are likely due, at least in part, to inexactness of the relaxation.

C. Comparison of Coefficients with Taylor Approximation

Fig. 5 compares the coefficients of the optimal linear approximation with those of the first-order Taylor approximation around the nominal operating point $(\mathbf{p}^*, \mathbf{q}^*)$ via the Root Mean Square (RMS) difference between the two sets of coefficients. The coefficients being compared represent ratios between power flows and power injections and thus the RMS error is a unitless quantity. The coefficients from the optimal approximation converge to those of the Taylor approximation as the radius R goes to zero, and the coefficients are very similar for small values of the radius (e.g., $R = 5\%$). This reinforces our interpretation of the optimal linear approximation
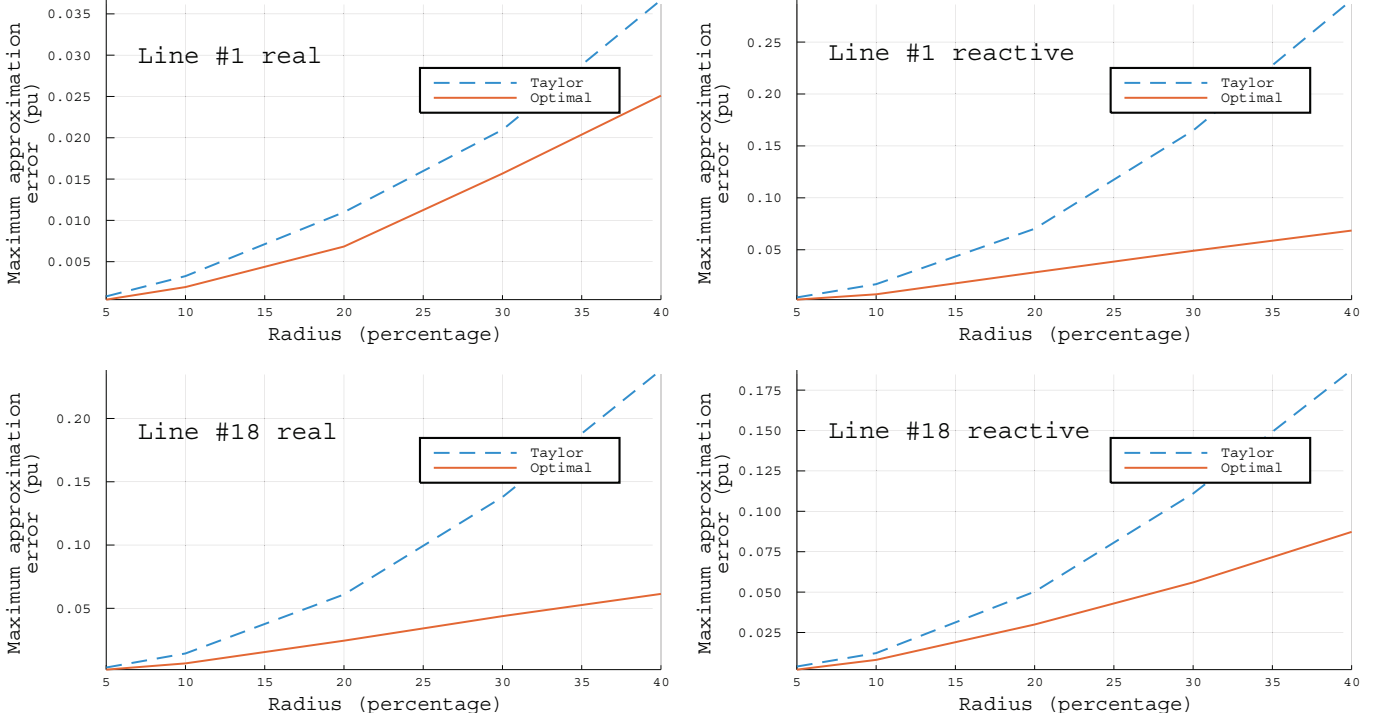
Fig. 3. Worst-case error of the optimal linear approximation obtained from *FindOptLin* and the first-order Taylor approximation for representative transmission lines #1 and #18 in the IEEE RTS 96 test case.
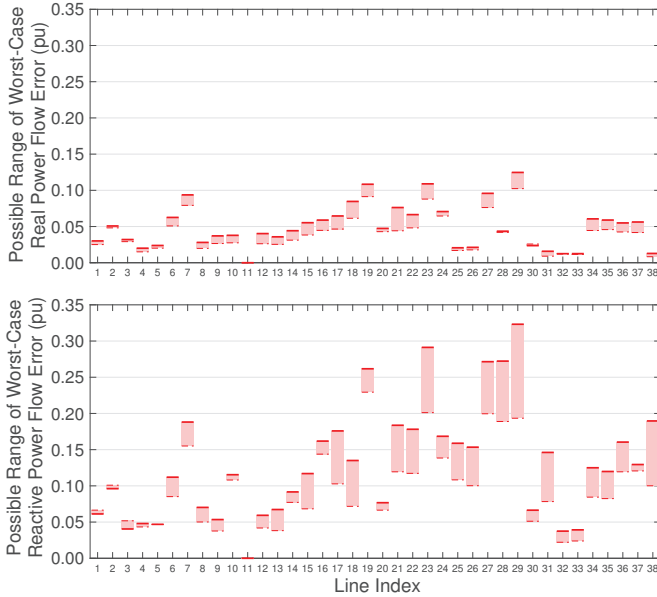

Fig. 4. Worst-case errors for real and reactive power flows on each line for the IEEE RTS 96 test case with a radius $R = 40\%$. The solid red lines are the upper bounds computed using a convex relaxation of (5) with $\mathbf{L} = (\ell_0, \ell_p, \ell_q)$ from the output of *FindOptLin*. The thin dashed red lines are the lower bounds computed by applying a local solver (Ipopt) to (5). The red regions between these bounds represent the potential values of the actual worst-case errors.

being an improvement over the Taylor approximation using the AC-PDTF matrix. The difference gets more significant for a large radius of $R = 40\%$. Even then, most of the coefficient values are quite close, with an RMS difference less than 0.01 for the real power approximation's coefficients. Despite the small differences, we obtain significant improvements (a factor

of four) in the real power approximation errors on certain lines.

D. Comparison Across Test Cases

Tables I and II present the results for four different test cases. The worst-case errors (given as averages over all lines and the maximum error for any line) for various sizes of the operating ranges, R, are shown. Values of errors below the tolerance of $\epsilon = 10^{-3}$ in *FindOptLin* are denoted as 0.000.

The approximation errors for the real power flows are systematically smaller than those for the reactive power flows. This agrees with the general intuition that reactive flows exhibit more non-linear behavior (see, for example, Fig. 1 in [21]). For both real and reactive power flows, the average approximation errors across all lines are significantly smaller than the maximum error, suggesting that the power flows on most of the lines are well approximated by the optimal linearizations. The growth of the computation time, shown in the last column, is primarily driven by the number of solves of the NLP (5).

V. CONCLUSION

This paper proposes a new approach for constructing linear power flow approximations that are both "adaptive" (tailored to specific systems and operating ranges of interest) and "optimal" (minimize an error metric relative to the non-linear AC power flow equations). These approximations are computed by formulating a bilevel optimization problem that is solved using a constraint generation algorithm. Empirical results demonstrate potential improvements of up to a factor of four over linearizations resulting from a first-order Taylor approximation. As discussed in Section III-C, our ongoing
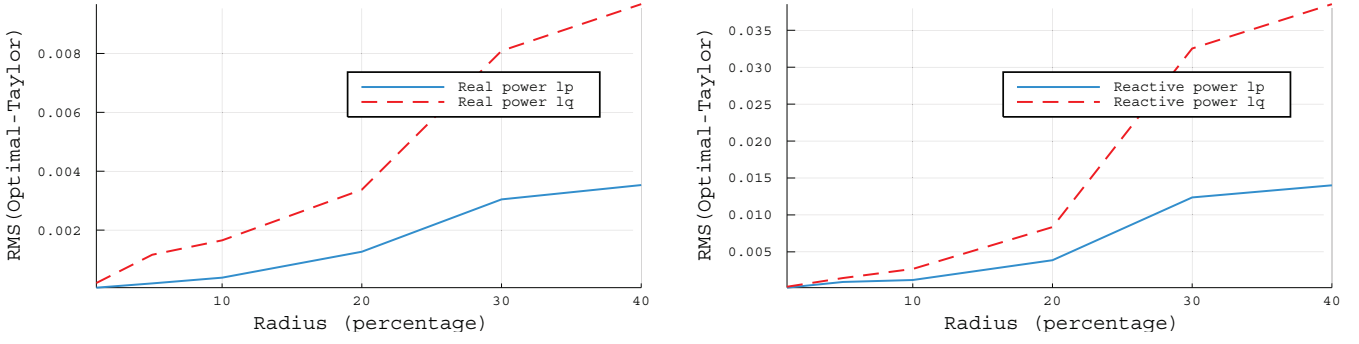
Fig. 5. The Root Mean Square (RMS) difference between the coefficient matrix of the first-order Taylor approximation and the optimal linearization for the IEEE RTS 96 test case. The RMS difference is a unitless quantity since the coefficients being compared are ratios between power flows and power injections.

TABLE I
WORST-CASE APPROXIMATION ERROR FOR REAL POWER FLOW OVER ALL TRANSMISSION LINES

System	Radius=10%		Radius = 20%		Radius = 30%		Radius = 40%		Radius = 40%, Taylor		Time
	Avg. error	Max. error	Avg. error	Max. error	Avg. error	Max. error	Avg. error	Max. error	Avg. error	Max. error	(sec.)
NESTA 14	0.000	0.000	0.000	0.001	0.000	0.002	0.000	0.004	0.002	0.008	3
RTS 96	0.003	0.008	0.012	0.032	0.025	0.068	0.039	0.102	0.079	0.243	25
NESTA 30	0.000	0.000	0.000	0.001	0.000	0.003	0.000	0.004	0.005	0.029	7
NESTA 57	0.000	0.002	0.002	0.010	0.004	0.020	0.007	0.035	0.019	0.089	80

TABLE II
WORST-CASE APPROXIMATION ERROR FOR REACTIVE POWER FLOW OVER ALL TRANSMISSION LINES

System	Radius=10%		Radius = 20%		Radius = 30%		Radius = 40%		Radius = 40%, Taylor		Time
	Avg. error	Max. error	Avg. error	Max. error	Avg. error	Max. error	Avg. error	Max. error	Avg. error	Max. error	(sec.)
NESTA 14	0.000	0.001	0.001	0.002	0.002	0.005	0.003	0.007	0.005	0.015	3
RTS 96	0.010	0.024	0.035	0.093	0.068	0.184	0.100	0.254	0.218	0.721	25
NESTA 30	0.000	0.001	0.001	0.002	0.002	0.005	0.002	0.009	0.011	0.037	8
NESTA 57	0.001	0.005	0.004	0.021	0.008	0.040	0.013	0.065	0.038	0.174	80

work is exploiting the flexibility inherent to the proposed approach in order to explore variants of the formulation presented here. Other ongoing work is performing comparisons to additional approximation techniques. We also aim to significantly improve computational speed using warm starts and a hybrid first- and second-order solution algorithm.

REFERENCES

[1] B. Stott, J. Jardim, and O. Alsaç, "DC Power Flow Revisited," *IEEE Trans. Power Syst.*, vol. 24, no. 3, pp. 1290–1300, Aug. 2009.
[2] M. E. Baran and F. F. Wu, "Optimal Capacitor Placement on Radial Distribution Systems," *IEEE Trans. Power Del.*, vol. 4, no. 1, pp. 725–734, Jan. 1989.
[3] D. K. Molzahn and I. A. Hiskens, "A Survey of Relaxations and Approximations of the Power Flow Equations," invited submission to *Found. Trends Electric Energy Syst.*, 2018.
[4] L. A. Roald, S. Misra, M. Chertkov, and G. Andersson, "Optimal Power Flow with Weighted Chance Constraints and General Policies for Generation Control," in *IEEE 54th Conf. Decis. Control (CDC)*, 2015, pp. 6927–6933.
[5] J. R. Martí, H. Ahmadi, and L. Bashualdo, "Linear Power-Flow Formulation Based on a Voltage-Dependent Load Model," *IEEE Trans. Power Del.*, vol. 28, no. 3, pp. 1682–1690, July 2013.
[6] H. Ahmadi, J. R. Martí, and A. von Meier, "A Linear Power Flow Formulation for Three-Phase Distribution Systems," *IEEE Trans. Power Syst.*, vol. 31, no. 6, pp. 5012–5021, Nov. 2016.
[7] A. Bernstein, C. Wang, E. Dall'Anese, J.-Y. Le Boudec, and C. Zhao, "Load-Flow in Multiphase Distribution Networks: Existence, Uniqueness, and Linear Models," *arXiv:1702.03310*, Feb. 2017.
[8] R. D. Zimmerman, C. E. Murillo-Sánchez, and R. J. Thomas, "MATPOWER: Steady-State Operations, Planning, and Analysis Tools for Power Systems Research and Education," *IEEE Trans. Power Syst.*, vol. 26, no. 1, pp. 12–19, 2011.
[9] A. J. Wood and B. F. Wollenberg, *Power Generation, Operation, and Control*. John Wiley & Sons, 2012.
[10] J. Y. Jackson, "Interpretation and Use of Generator Reactive Capability Diagrams," *IEEE Trans. Ind. General Appl.*, vol. IGA-7, no. 6, pp. 729–732, Nov. 1971.
[11] D. K. Molzahn, B. C. Lesieutre, and C. L. DeMarco, "Approximate Representation of ZIP Loads in a Semidefinite Relaxation of the OPF Problem," *IEEE Trans. Power Syst.*, vol. 29, no. 4, pp. 1864–1865, July 2014.
[12] D. K. Molzahn, "Incorporating Squirrel-Cage Induction Machine Models in Convex Relaxations of OPF Problems," *IEEE Trans. Power Syst.*, vol. 32, no. 6, pp. 4972–4974, Nov. 2017.
[13] A. Wächter and L. T. Biegler, "On the Implementation of a Primal-Dual Interior Point Filter Line Search Algorithm for Large-Scale Nonlinear Programming," *Math. Prog."*, vol. 106, no. 1, pp. 25–57, 2006.
[14] K. Dvijotham and D. K. Molzahn, "Error Bounds on the DC Power Flow Approximation: A Convex Relaxation Approach," in *IEEE 55th Conf. Decis. Control (CDC)*, 2016, pp. 2411–2418.
[15] C. Josz and D. Molzahn, "Multi-Ordered Lasserre Hierarchy for Large Scale Polynomial Optimization in Real and Complex Variables," to appear in *SIAM J. Optimiz.*, 2018.
[16] C. Coffrin, H. L. Hijazi, and P. Van Hentenryck, "The QC Relaxation: A Theoretical and Computational Study on Optimal Power Flow," *IEEE Trans. Power Syst.*, vol. 31, no. 4, pp. 3008–3018, July 2016.
[17] ——, "Strengthening the SDP Relaxation of AC Power Flows with Convex Envelopes, Bound Tightening, and Valid Inequalities," *IEEE Trans. Power Syst.*, vol. 32, no. 5, pp. 3549–3558, Sept. 2017.
[18] C. Coffrin, D. Gordon, and P. Scott, "NESTA, The NICTA Energy System Test Case Archive," *arXiv:1411.0359*, Aug. 2016.
[19] Los Alamos National Laboratory, Advanced Network Science Initiative, "PowerModels.jl," https://github.com/lanl-ansi/PowerModels.jl.
[20] I. Dunning, J. Huchette, and M. Lubin, "JuMP: A modeling language for mathematical optimization," *SIAM Rev.*, vol. 59, no. 2, pp. 295–320, 2017.
[21] C. Coffrin and P. Van Hentenryck, "A Linear-Programming Approximation of AC Power Flows," *INFORMS J. Comput.*, vol. 26, no. 4, pp. 718–734, 2014.